Anti-tumor properties of FoxO1 in YD-9 oral squamous cell carcinoma cells

YU GYUNG KIM[1*], CHAEEUN SEONG[1*], KYOUNG-AH CHO[2*], SANG MIN LEE[1], TAE-JUN KIM[1], HYEON JI KIM[1], JIN-HWA CHO[1], WON JUNG[3], SUNGIL JANG[4], JAE-CHEON SHIN[5], KYUNG-HA LEE[6], JIN-SEOK BYUN[2] and DO-YEON KIM[1]

Departments of [1]Pharmacology and [2]Oral Medicine, School of Dentistry, Kyungpook National University, Daegu 41940; Departments of [3]Oral Medicine and [4]Oral Biochemistry, Institute of Oral Bioscience, School of Dentistry, Jeonbuk National University, Jeonju 54896; [5]Advanced Bio-Convergence Center, Pohang Technopark, Pohang 37668; [6]Department of Molecular Biology, Pusan National University, Busan 46241, Republic of Korea

Received December 16, 2022; Accepted March 7, 2023

DOI: 10.3892/or.2023.8559

Abstract. Oral squamous cell carcinoma (OSCC) is a tumor with a poor prognosis and a high recurrence rate. Despite its high annual incidence worldwide, appropriate therapeutic strategies have not yet been developed. Consequently, the 5-year survival rate for OSCC is low when advanced stages or recurrence is diagnosed. Forkhead transcriptional factor O1 (FoxO1) is a key mediator for maintaining cellular homeostasis. FoxO1 can function as a tumor suppressor as well as an oncogene depending on the cancer type. Therefore, the precise molecular functions of FoxO1 need to be validated, considering intracellular factors and the extracellular environment. To the best of our knowledge, however, the roles of FoxO1 in OSCC have not yet been defined. The present study examined FoxO1 levels under pathological conditions (oral lichen planus and oral cancer) and selected an appropriate OSCC cell line (YD-9). Crispr/Cas9 was used to generate FoxO1-deficient YD-9 cells in which the protein levels of phospho ERK and phospho STAT3 were upregulated, promoting cancer proliferation and migration. In addition, FoxO1 reduction increased the levels of the cell proliferation markers phospho H3 (Ser10) and PCNA. FoxO1 loss significantly reduced cellular ROS levels and apoptosis in YD-9 cells. Collectively, the present study demonstrated that FoxO1 exerted an anti-tumor effect by suppressing proliferation and migration/invasion but promoting oxidative stress-linked cell death in YD-9 OSCC cells.

Correspondence to: Professor Do-Yeon Kim, Department of Pharmacology, School of Dentistry, Kyungpook National University, 2177 Dalgubeoldae, Jung, Daegu 41940, Republic of Korea
E-mail: dykim82@knu.ac.kr

Professor Jin-Seok Byun, Department Oral Medicine, School of Dentistry, Kyungpook National University, 2177 Dalgubeoldae, Jung, Daegu 41940, Republic of Korea
E-mail: jsbyun@knu.ac.kr

*Contributed equally

Key words: forkhead transcriptional factor O1, oral squamous cell carcinoma, proliferation, reactive oxygen species

Introduction

Oral squamous cell carcinoma (OSCC) is one of the most common types of head and neck SCC (HNSCC), accounting for more than half of HNSCC cases. OSCC originates in the squamous epithelium of the dental area (1). It is an aggressive neoplasia with a poor prognosis and a high recurrence rate (2). Despite progress in anti-cancer therapeutic research, the 5-year survival rate for OSCC has remained at 30% when detected at advanced stages (3). Notably, the mortality rate of patients with OSCC increases up to 92% when recurrence is diagnosed (4). Therefore, detailed pathogenic mechanisms need to be identified.

For tumorigenesis, multiple critical steps are required. First, cancer cells sustain autonomous proliferative capacity that is maintained to avoid senescence that can be caused by excessive cell proliferation (5). Second, cancer cells effectively resist cell death by regulating the apoptotic machinery. Apoptosis initiation can be negatively controlled by pro-survival members of the Bcl-2 family. Third, carcinoma cells promote local invasion and distant metastasis by activating epithelial-mesenchymal transition and/or invasion-inducing signals. Additionally, cancer cells have the potential for replicative immortality, angiogenesis, evading growth suppressors, reprogramming cellular metabolism and inhibiting eradication by the immune system (6). Therefore, key molecules involved in these tumor hallmarks must be identified to develop anti-tumor therapeutic strategies.

Forkhead transcriptional factor O1 (FoxO1) is a critical gene for regulating cellular homeostasis. FoxO1 controls the expression of target genes responsible for redox balance, cell proliferation, inflammation, metabolism and apoptosis. FoxO1 has been regarded as a putative tumor suppressor in numerous

types of neoplasms (7). Several *in vitro* and *in vivo* studies have shown that FoxO1 suppresses cancer cell proliferation and induces apoptosis (8). FoxO1 also exerts anti-tumor effects by inhibiting invasion and angiogenesis (9,10). Consistent with these previous findings, FoxO1 is downregulated, mutated or inactivated in numerous cancers (11). However, it has also been demonstrated that FoxO1 supports cancer progression; gain of function mutations in FoxO1 have been reported in specific cancer types (12). Furthermore, the concurrent downregulation of FoxO1 and FoxO3 inhibits tumor growth and metastasis (13). To the best of our knowledge, however, the molecular functions of FoxO1 in OSCC have not yet been investigated. Therefore, the present study aimed to explore the potential intracellular roles of FoxO1 in OSCC.

Materials and methods

Plasmid construction. The lentiCRISPRv2 plasmid, a gift from Dr Feng Zhang (Addgene, Inc.; cat. no. 52961) (14), was digested with *Bsm*BI (New England BioLabs, Inc.) according to the manufacturer's instructions, followed by dephosphorylation and gel purification. For genetic perturbation of FoxO1, a pair of oligos (5'-CACCGGTTGCCCCACGCGTTGCGG C-3' and 5'-AAACGCCGCAACGCGTGGGGCAACC-3'; Macrogen) were phosphorylated, annealed at 60˚C for 30 sec and ligated into the digested lentiCRISPRv2 plasmid, which was called LC-FoxO1.

Cell culture and generation of FoxO1-deficient cells. YD-9, YD-8, FaDu, and SNU1041 cells were purchased from Korean Cell line bank. YD-9, YD-8, and SNU1041 cells were maintained in RPMI-1640 medium (Gibco; Thermo Fisher Scientific, Inc.), and FaDu cells were maintained in MEM (Cytiva), supplemented with 10% fetal bovine serum (Gibco; Thermo Fisher Scientific, Inc.) and 1% penicillin-streptomycin in a humidified atmosphere containing 5% CO_2 at 37˚C. To generate FoxO1-decifient cells, the 0.5 μg of LC-FoxO1 construct was transfected into YD-9 cells via electroporation (pulse voltage: 1400 V, pulse width: 20 ms, pulse number: 2) using the Neon Transfection System (Invitrogen; Thermo Fisher Scientific, Inc.), according to the manufacturer's instructions. YD-9 cells transfected with GFP-targeting plasmid were used as control cells. After 2 days of transfection, the cells were selected with 2 μg/ml puromycin. Puromycin-resistant control and FoxO1-deficient cells were maintained in RPMI-1640 supplemented with 10% fetal bovine serum, 1% penicillin-streptomycin and 2 μg/ml puromycin. To assess the effect of FoxO1 on YD-9 cell survival, control and FoxO1-deficient YD-9 cells were treated with 10 ng/ml TNFα for 2 days.

Clinical samples. A total of seven (two males and 5 females) randomized Korean patients diagnosed with oral lichen planus (OLP) (age range: 47-62 years old) from April to July 2022 in the Department of Oral Medicine, Jeonbuk National University Hospital (Jeonju, Korea) were enrolled in the study. The inclusion criteria were reticular/atrophic/erosive OLP verified according to the clinicopathological criteria by World Health Organization (WHO) (15), including visual validation of whitish and erythematous mucosal lesions on the buccal mucosa and confirmation using incisional biopsy. The following diseases and systemic conditions were excluded, such as autoimmune diseases including psoriasis and rheumatoid arthritis, other oral mucosal infectious diseases including oral candidiasis and herpes virus infection, and oral cancers. The present study was approved by the Institutional Review Board of Jeonbuk National University Hospital (approval no. CUH 2021-02-044-001), and written informed consent was obtained from all the participants.

Protein preparation and immunoblot analysis. YD-9 cells were directly disrupted in laemmli buffer [60 mM Tris-HCl (pH 6.8), 2% (w/v) sodium dodecyl sulfate (SDS), 10% (v/v) glycerol and 0.02% (w/v) bromophenol blue], followed by sonication and heat denaturation. Samples were separated on 12% SDS-polyacrylamide gels, and proteins were transferred to a polyvinylidene fluoride membrane. After being blocked with 5% skimmed milk at room temperature for 30 min, the membranes were incubated overnight at 4˚C with the following primary antibodies against phosphorylated (phospho) H3 at Ser 10 (1:1,000, #9701, Cell Signaling Technology, Inc.), total H3 (1:50,000, ab1791, Abcam), PCNA (1:1,000, BS1289, Bioworld Technology, Inc.), cyclin B (1:200, sc-245, Santa Cruz Biotechnology, Inc.), ARF (1:1,000, PA1-127, Thermo Fisher Scientific, Inc.), CDK5 (1:1,000, CSB-PA005067LA01HU, Cusabio Technology, LLC), β actin (1:50,000, A5316, Sigma-Aldrich; Merck KGaA), PRDX5 (peroxiredoxin 5) (1:1,000, A305-339A, Bethyl Laboratories, Inc.), PRDX3 (1:1,000, A304-744A, Bethyl Laboratories, Inc.), LC3 (1:1,000, NB100-2220, Novus Biologicals, LLC), HIF1α (1:1,000, ab82832, Abcam), SQSTM1 (Sequestosome1)/p62 (1:1,000, cat. no. ab56416, Abcam), Beclin 1 (1:1,000, A302-566A, Bethyl Laboratories, Inc.), survivin (1:1,000, #2808, Cell Signaling Technology, Inc.), total JNK (1:1,000, #9252, Cell Signaling Technology, Inc.), total ERK (1:1,000, #4695, Cell Signaling Technology, Inc.), total NFκB (1:1,000, #8242, Cell Signaling Technology, Inc.), phospho JNK (1:1,000, #4668, Cell Signaling Technology, Inc.), phospho ERK (1:1,000, MA5-15174, Thermo Fisher Scientific, Inc.), and phospho NFκB (1:1,000, MA5-15160, Thermo Fisher Scientific, Inc.). The membranes were incubated at room temperature for 1 h with secondary anti-rabbit (1:5,000, ab205718, Abcam) and anti-mouse (1:10,000, A90-116P, Bethyl Laboratories, Inc.) antibodies that were horseradish peroxidase conjugated. Immunoreactive signals were detected using the D-Plus™ ECL Femto system (ECL-FS200, Donginbiotech Co., Ltd., Korea) and Fusion Solo S chemiluminescence imaging system (Vilber). Densitometric analysis of western blot bands was carried out using ImageJ software (National Institutes of Health).

Reactive oxygen species (ROS) detection. Intracellular ROS levels were determined using the fluorogenic CellROX® Orange reagent (Invitrogen; Thermo Fisher Scientific, Inc.) according to the manufacturer's instructions. CellROX reagent was added to cultured cells at a final concentration of 5 μM for 30 min at 37˚C. Nuclear DAPI staining was conducted with NucBlue Live ReadyProbes Reagent (Invitrogen; Thermo Fisher Scientific, Inc.) for 5 min. Fluorescent microscopic images were acquired using the EVOS FL Auto Imaging System (Thermo Fisher Scientific, Inc.) (magnification, x200).

Immunofluorescence. OLP tissues were fixed with 10% formalin at room temperature for 24 h. Paraffin-embedded OLP tissue sections were cut at 5-8 μm thickness and incubated at 55˚C for 30 min before staining. Two changes of xylene (10 min each) were used to dewax the tissue sections and 100, 90, 80, 70 and 50% ethanol, and water (10 min each) were used for hydration. Following deparaffinization and hydration, the OLP tissue sections were incubated with blocking serum (1% bovine serum albumin, 4% normal goat serum and 0.2% Triton X-100 in PBS) (Vector Laboratories, Inc.) for 2 h at room temperature and subsequently treated with primary antibody against FoxO1 (1:200, ab39670, Abcam) overnight at 4˚C. The next day, sections were rinsed with PBS and incubated with Alexa Fluor® 555 (1:1,000, ab150078, Abcam) for 90 min at room temperature. Fluorescent microscopic images were acquired using the EVOS FL Auto Imaging System (Thermo Fisher Scientific, Inc.) (magnification, x100).

Reverse transcription-quantitative (RT-q)PCR. Total RNA was extracted from YD-9 cells using a FavorPrep™ Blood/Cultured Cell Total RNA Kit (Favorgen Biotech Corporation), according to the manufacturer's instructions. A total of 300 ng total RNA was treated with RNase-free DNase (Sigma-Aldrich; Merck KGaA) for 15 min, followed by inactivation of DNase with EDTA treatment and heating. Total RNA was reverse-transcribed into cDNA using the First Strand cDNA Synthesis kit (Thermo Fisher Scientific, Inc.), according to the manufacturer's instructions. RT-qPCR was performed on cDNA samples with the Luna® Universal qPCR Master Mix (New England BioLabs, Inc.) using the Mic qPCR Cycler (Bio Molecular Systems). The thermocycling conditions were as follows: Initial denaturation at 95˚C for 1 min was followed by cycles comprising denaturation at 95˚C for 15 sec, annealing and extension at 60˚C for 30 sec. The relative mRNA expression was calculated via the $2^{-\Delta\Delta Cq}$ method (16). The sequences of the forward and reverse primers are presented in Table I.

Table I. Forward and reverse primers used for reverse transcription-quantitative PCR.

Gene	Sequence, 5'→3'
hRPL32 (F)	GAAGTTCCTGGTCCACAACG
hRPL32 (R)	GCGATCTCGGCACAGTAAG
hKRT76 (F)	CCGCAGAGAATGAGTTTGTGGG
hKRT76 (R)	CATAGAGGGTCCTCAGGAAGCT
hKRT80 (F)	CTCAATGTGCGCATCCAGAAGC
hKRT80 (R)	TTGGTCTTGGCATCCTGGAAGG
hKRT23 (F)	GGTGACATCCACGAACTGAAGC
hKRT23 (R)	AGCTTGCAGGAGTACCGAGACT
hKRT10 (F)	CCTGCTTCAGATCGACAATGCC
hKRT10 (R)	ATCTCCAGGTCAGCCTTGGTCA
hTNFα (F)	AGCCCATGTTGTAGCAAACC
hTNFα (R)	TGAGGTACAGGCCCTCTGAT
hCCL20 (F)	TGCTGTACCAAGAGTTTGCTC
hCCL20 (R)	CGCACACAGACAACTTTTTCTTT

RPL, ribosomal protein L; KRT, keratin; CCL, chemokine (C-C motif) ligand; F, forward; R, reverse.

Colony formation assay. LC-GFP and LC-FoxO1 cells were seeded in 6-well plates at a density of 500 cells/well and incubated at 37˚C for 14 days. After incubation, the wells were washed twice with PBS, fixed with 4% paraformaldehyde at room temperature for 15 min. Cells were stained with 0.1% crystal violet at RT for 30 min and then lysed with 1% SDS. Quantitative changes in clonogenicity was assessed at OD570 nm by spectrometer.

Bioinformatics data analysis. Analysis of the FoxO1 Expression in the HNSCC was performed using cBioPortal (cbioportal.org), a publicly available database for tumor transcriptomics. Gene Expression Profiling Interactive Analysis (gepia.cancer-pku.cn) was used to compare FoxO1 gene expression among cancer types and tumor stages. Transcriptome datasets from the National Center for Biotechnology Information Gene Expression Omnibus (ncbi.nlm.nih.gov/geo/) were utilized to assess FoxO1 transcript levels in OSCC. G:Profiler (http://biit.cs.ut.ee/gprofiler/gost) was utilized to perform gene ontology (GO) enrichment analysis for the biological process on gene sets.

Transwell migration assay. A 24-well Transwell insert system with an 8.0 μm pore size polycarbonate membrane was purchased from Corning, Inc. 10% FBS-containing RPMI was placed in the lower chambers to as a chemoattractant. LC-GFP and LC-FoxO1 cells ($5x10^4$ cells/insert) in 300 μl serum-free RPMI medium were treated with 200 nM $CoCl_2$ at 37˚C for 12 h, seeded in the upper chamber and allowed to migrate at 37˚C for 24 h. The cells were fixed with 4% paraformaldehyde at RT for 15 min and stained with 0.1% crystal violet at room temperature for 20 min. Non-migrated cells were removed from the top of each insert using a cotton swab. Fluorescent microscopic images were acquired using the EVOS FL Auto Imaging System (Thermo Fisher Scientific, Inc.; magnification, x100).

Wound healing assay. The migration ability of YD-9 cells was measured using wound healing assay. YD-9 cells were suspended in serum-free RPMI and stained with 5 μl/ml 1,1'-dioctadecyl-3,3,3',3'-tetramethylindocarbocyanine perchlorate) 37˚C for 30 min. Cells were washed with PBS and seeded in 12-well plates at a density of $1x10^5$ cells/well. When cells grew to ~100% confluency in a monolayer, a scratch was made using a 1,000 μl pipette tip. After removing cell debris by washing three times with PBS, the cells were incubated with RPMI containing 10% FBS at 37˚C. Images were acquired at the 0, 6, 12 and 24 h post-scratching. Fluorescent microscopic images were acquired using the EVOS FL Auto Imaging System (Thermo Fisher Scientific, Inc.; magnification, x100).

Statistical analysis. Unpaired two-tailed Student's t test was used for experiments comparing two groups. One-way ANOVA followed by post hoc Bonferroni's correction was used to assess >2 groups. All data are expressed as the mean ± SEM of ≥3 independent experimental repeats. GraphPad Prism software (version 9; GraphPad Software, Inc.; Dotmatics) was used for all statistical analyses. $P<0.05$ was considered to indicate a statistically significant difference.

Results

Analysis of FoxO1 expression in premalignant and malignant lesions. To explore the potential roles of FoxO1 in the pathogenesis of OSCC, expression of FoxO1 was assessed. Previously, Shi *et al* (17) performed transcriptome profiling with clinical samples and demonstrated that FoxO1 mRNA levels are significantly increased in both OLP, a premalignant lesion, and OSCC. The present immunofluorescence staining of normal and OLP samples validated that FoxO1 protein expression was significantly upregulated in both reticular and ulcerative forms of OLP compared with normal tissue (Fig. 1A).

To analyze FoxO1 expression levels in OSCC, publicly available gene expression datasets were used. According to the data from The Cancer Genome Atlas and cBioPortal (18,19), abnormal FoxO1 expression was detected in 2.7% of HNSCC cases. FoxO1 upregulation was more common than FoxO1 downregulation (Fig. 1B). Gene Expression Profiling Interactive Analysis (gepia.cancer-pku.cn/) was used to compare FoxO1 gene expression in cancer types. By contrast to other cancer types in which FoxO1 was downregulated, FoxO1 expression was not altered in HNSCC (Fig. 1C) (20). The expression of FoxO1 varied during tumor progression (Fig. 1D). FoxO1 transcript levels were assessed in two oral cancer datasets (accession nos. GSE74530 and GSE51010) from the National Center for Biotechnology Information Gene Expression Omnibus profile database. Although the clinical sample number was insufficient to draw a general conclusion, FoxO1 was significantly upregulated in OSCC (Fig. 1E).

FoxO1 protein levels were assessed in four HNSCC (including OSCC) cell lines. Compared with normal human oral keratinocytes, FoxO1 protein was upregulated in FaDu and YD-9 cells but downregulated in YD-8 and SNU1041 cells (Fig. 1F), suggesting that FoxO1 expression was increased in a subpopulation of patients with OSCC. To determine the molecular function of FoxO1 in OSCC, YD-9 was selected as a cell model. YD-9 is a human papillomavirus DNA-negative OSCC acquired from buccal mucosa where premalignant OLP frequently occurs. As FoxO1 is overexpressed in both OLP and YD-9 cells, the present study explored the pathophysiological roles of FoxO1 in OLP and OSCC. Compared with the other HNSCC three cell lines that contain the mutant form of p53, YD-9 cells express wild-type p53. Therefore, molecular function of FoxO1 could be determined excluding the effect of the p53 mutation (21).

FoxO1 inhibits proliferation in YD-9 human OSCC cells. To determine the disrupted intracellular biological processes in OSCC, Gene Ontology (GO) enrichment analysis of transcriptome data (accession no. GSE70665) was performed (22-24). As a result, 1,890 genes (687 up- and 1,203 downregulated) were differentially expressed in OSCC compared with normal samples. Upregulated genes were highly enriched in 'keratinization' and 'cell division' (Fig. S1).

To determine whether FoxO1 was involved in the keratinization process, FoxO1 expression was knocked out in YD-9 cells using Crispr/Cas9 (LC-FoxO1; Fig. 2A). mRNA levels of keratin (KRT) genes were up-(KRT23) or downregulated (KRT76, KRT80 and KRT10) following FoxO1 silencing (Fig. 2B). It was previously reported that certain KRT genes are involved in tumor growth. While KRT23 promotes cancer proliferation (25), KRT76 and KRT10 suppress cancer growth (26,27), raising the possibility that FoxO1 could regulate cell proliferation. FoxO1 reduction increased the levels of the cell proliferation markers phospho H3 (Ser10) and PCNA (Fig. 2C). In addition, FoxO1 depletion led to upregulation of cell cycle-promoting factors Cyclin B and CDK5 and downregulation of the ARF tumor suppressor (Fig. 2C). In line with a previous report that ERK and STAT3 signaling are key for OSCC proliferation (28), FoxO1 deficiency increased the ERK and STAT3 phosphorylation (Fig. 2D). The enhancement of cell proliferation by FoxO1 silencing was validated by time-dependent changes in the total live cell counts (Fig. 2E). Furthermore, FoxO1 deficiency increased clonogenicity (Fig. 2F). Collectively, these data suggested that FoxO1 served an anti-proliferative function in OSCC pathogenesis.

FoxO1 suppresses migration in YD-9 human OSCC cells. As simultaneous activation of ERK and STAT3 signaling is key for the migration/invasion and proliferation of cancer cells (29), it was investigated with FoxO1 was implicated in the migration of YD-9 cells. *In vitro* wound healing assay demonstrated that FoxO1-disrupted cells showed higher migration capacity than control cells (Fig. 3A and B). Transwell migration assay showed that FoxO1-deficient cells had higher migration capacity than control cells. When cell migration was stimulated with $CoCl_2$, LC-FoxO1 cells exhibited stronger migration potential than control cells (Fig. 3C and D). Consistently, increased phosphorylation of ERK and STAT3 following FoxO1 silencing was maintained when cells were treated with $CoCl_2$ (Fig. 3E and F). These data suggest that FoxO1 served an inhibitory function in the migration of OSCC cells.

FoxO1 silencing decreases oxidative stress and apoptosis in YD-9 cells. FoxO1 is implicated in the oxidative stress response (30). In addition, oxidative stress is involved in numerous disorders, including OLP and OSCC (31). To assess the effect of FoxO1 depletion on intracellular oxidative stress, ROS levels were determined by CellROX staining in control and FoxO1-deficient cells. Intracellular ROS levels significantly decreased following FoxO1 silencing (Fig. 4A).

Peroxiredoxins (PRDXs) are key factors contributing to ROS scavenging. *PRDX3* and *PRDX5* mRNA expression is regulated by FoxO family members (32,33). Although the PRDX3 protein expression was not changed by FoxO1 deficiency, PRDX5 was notably upregulated by FoxO1 disruption, which could partly explain the decreased ROS levels in the LC-FoxO1 cells (Fig. 4B). Considering the interplay between autophagy and oxidative stress (34), autophagic flux following FoxO1 silencing was assessed. However, we could not observe any signature of autophagy activation/suppression by FoxO1 depletion in YD-9 cells, which was determined by the unchanged LC3 level (Fig. 4C).

As inflammation promotes OSCC pathogenesis, the effect of FoxO1 on the intracellular inflammatory response was assessed. As expected, the phosphorylation of JNK and NFκB was increased by TNFα stimulation. However, none of JNK and NFκB pathways seemed to be affected by FoxO1 perturbation (Fig. S2A). Consistently, mRNA levels of the

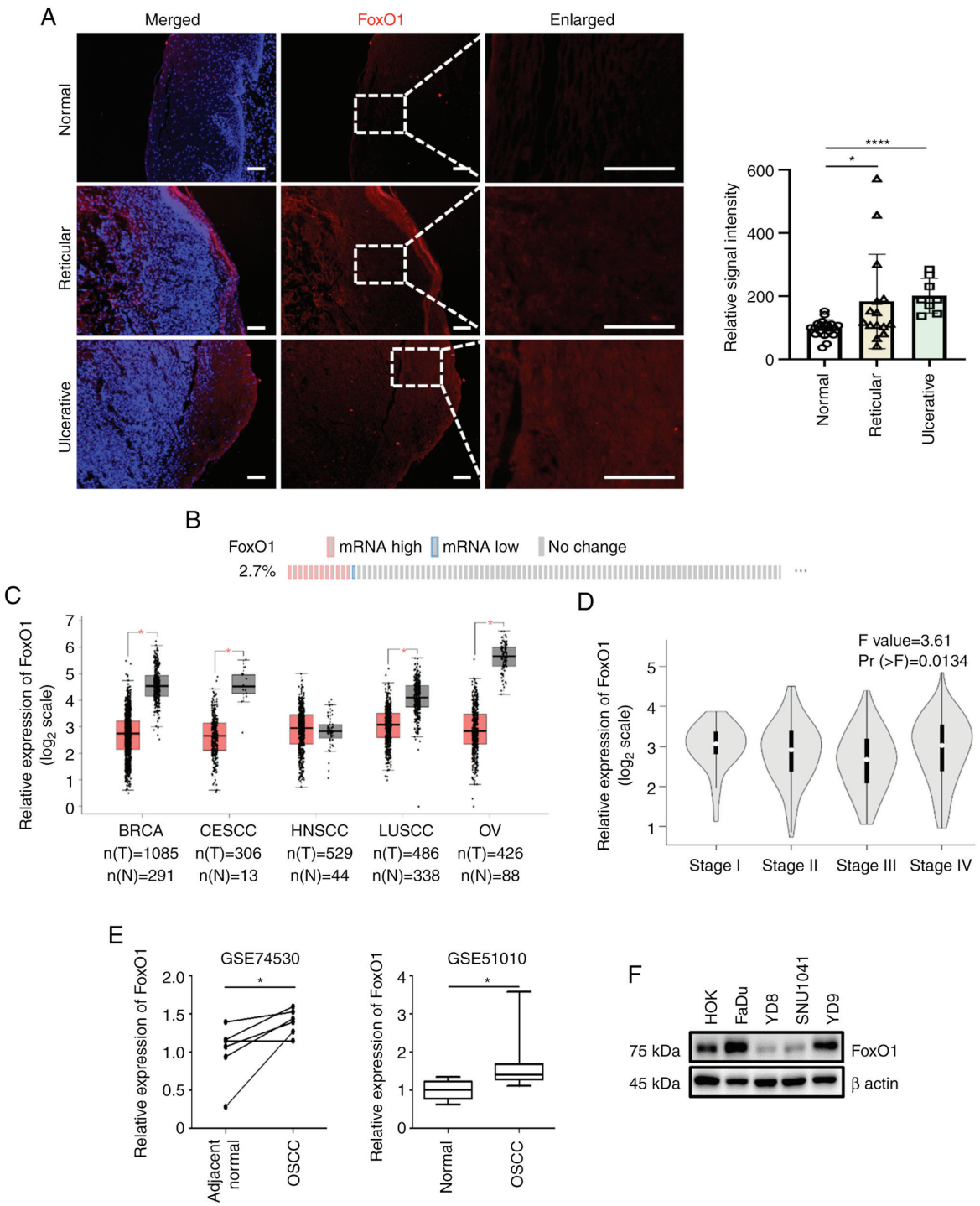

Figure 1. FoxO1 expression profile. (A) Normal and reticular- and ulcerative-type oral lichen planus samples were immunostained with FoxO1 antibody (red). Nuclear DAPI staining is shown in blue. Scale bar, 50 μm. Relative FoxO1 fluorescence intensities are shown. (B) Alteration of FoxO1 expression in HNSCC. The number of patients with HNSCC with upregulated (red) or downregulated (blue) expression of FoxO1 is presented. Data were derived from cBioPortal (cbioportal.org). (C) Expression levels of FoxO1 in cancer were evaluated via Gene Expression Profiling Interactive Analysis. (D) FoxO1 expression based on pathological HNSCC stage. (E) Comparison of FoxO1 mRNA expression between N and OSCC cells. Data were extracted from the National Center for Biotechnology Information Gene Expression Omnibus profile database. (F) Immunoblot analysis of FoxO1 protein. β actin was used as a loading control. BRCA, breast invasive carcinoma; CESCC, cervical squamous cell carcinoma and endocervical adenocarcinoma; LUSCC, lung squamous cell carcinoma; OV, ovarian serous cystadenocarcinoma; FoxO1, forkhead transcriptional factor O1; HNSCC, head and neck squamous cell carcinoma; OSCC, oral squamous cell carcinoma; T, tumor; N, normal. *P<0.05, ****P<0.0001.

pro-inflammatory genes TNFα and CC Motif Chemokine Ligand 20 were clearly induced by TNFα but those were unchanged by FoxO1 perturbation (Fig. S2B), suggesting that FoxO1 exerted a negligible effect on the acute inflammatory response in YD-9 cells.

A strong intracellular inflammatory status contributes to tumor cell death (35). YD-9 cells were treated with TNFα for 2 days before measurement of cell survival. Exposure to TNFα significantly decreased YD-9 cell survival. However, FoxO1 deficiency effectively suppressed OSCC cell death (Fig. 4D).

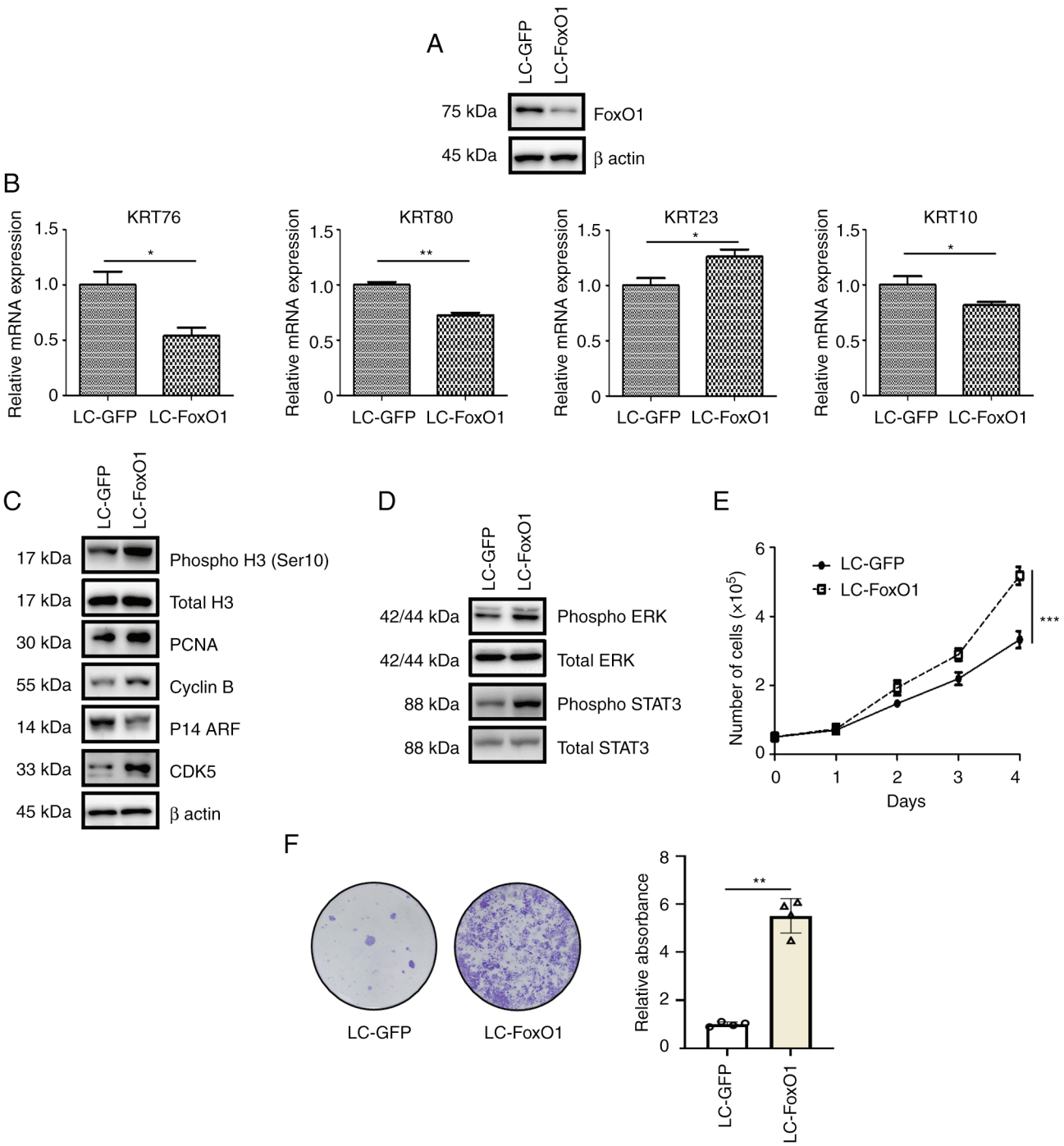

Figure 2. FoxO1 deficiency increases YD-9 cell proliferation. (A) Genetic perturbation of FoxO1 in YD-9 cells was confirmed via immunoblot analysis. (B) mRNA expression of genes in control (LC-GFP) and FoxO1-deficient (LC-FoxO1) cells. (C) Western blot analysis of cell cycle-associated proteins in control and FoxO1-deficient cells. β actin was used as loading control. (D) Immunoblot analysis of phosphoproteins in control and FoxO1-deficient cells. (E) Total cell numbers at 1-4 days after cell seeding. (F) Colony formation assay. Control and FoxO1-deficient cells were grown for 14 days and stained with crystal violet. Colonies were quantified by measuring the absorbance of crystal violet at 570 nm. FoxO1, forkhead transcriptional factor O1; KRT, keratin; phospho, phosphorylated. *P<0.05, **P<0.01, ***P<0.001.

Consistent with this data, Survivin and Bcl-xL protein levels remained high in FoxO1-deficient cells (Fig. 4E and F), again indicating the anti-tumor role of FoxO1 in YD-9 OSCC (Fig. 4G).

Discussion

Unlike other tumor types where FoxO1 is downregulated, in the present study, FoxO1 transcript abundance was unchanged or increased in some populations of OSCC. Expression enhancement of specific genes during pathogenesis may indicate that these genes promote progression of disease. Alternatively, cells could operate defensive mechanisms by upregulating specific genes that have suppressive roles in the pathogenesis of disease. The present results support the latter by showing that FoxO1 had suppressive roles in proliferation and migration but promoted cell death in OSCC.

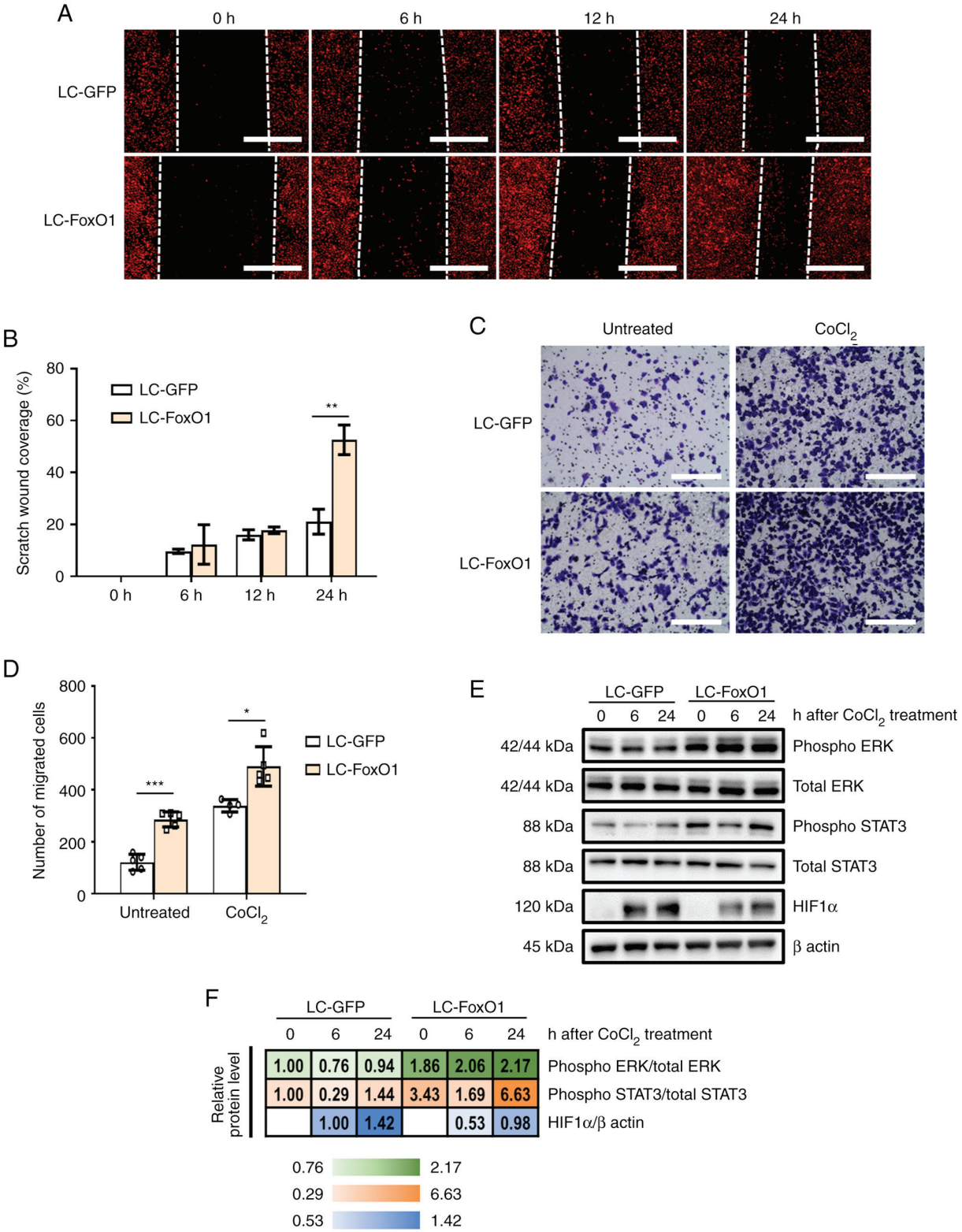

Figure 3. FoxO1 deficiency increases the migration potential of YD-9 cells. (A) Representative images of wound healing assay of control and FoxO1-deficient cells. Scale bar, 50 μm. (B) Quantification of wound healing rate. (C) Representative images of Transwell migration assay of control and FoxO1-deficient cells. Scale bar, 50 μm. (D) Quantification of migration rate. (E) Immunoblot analysis of phospho ERK, phospho STAT3 and HIF1α proteins in control and FoxO1-deficient cells. β actin was used as the loading control. (F) Quantification of immunoblot analysis. FoxO1, forkhead transcriptional factor O1; HIF, hypoxia-inducible factor; phospho, phosphorylated. *P<0.05, **P<0.01, ***P<0.001.

In line with the present study, FoxO1 is regarded as a tumor suppressor. FoxO1 is highly expressed in non-Hodgkin lymphoma and constitutive activation of FoxO1 inhibits proliferation and promotes cell cycle arrest/apoptosis (36). In prostate cancer, the reduction of FoxO1 activity and expression increases cancer cell proliferation (37). FoxO1 deficiency decreases cell death in response to energy stress (38). On the other hand, however, studies have demonstrated that FoxO1

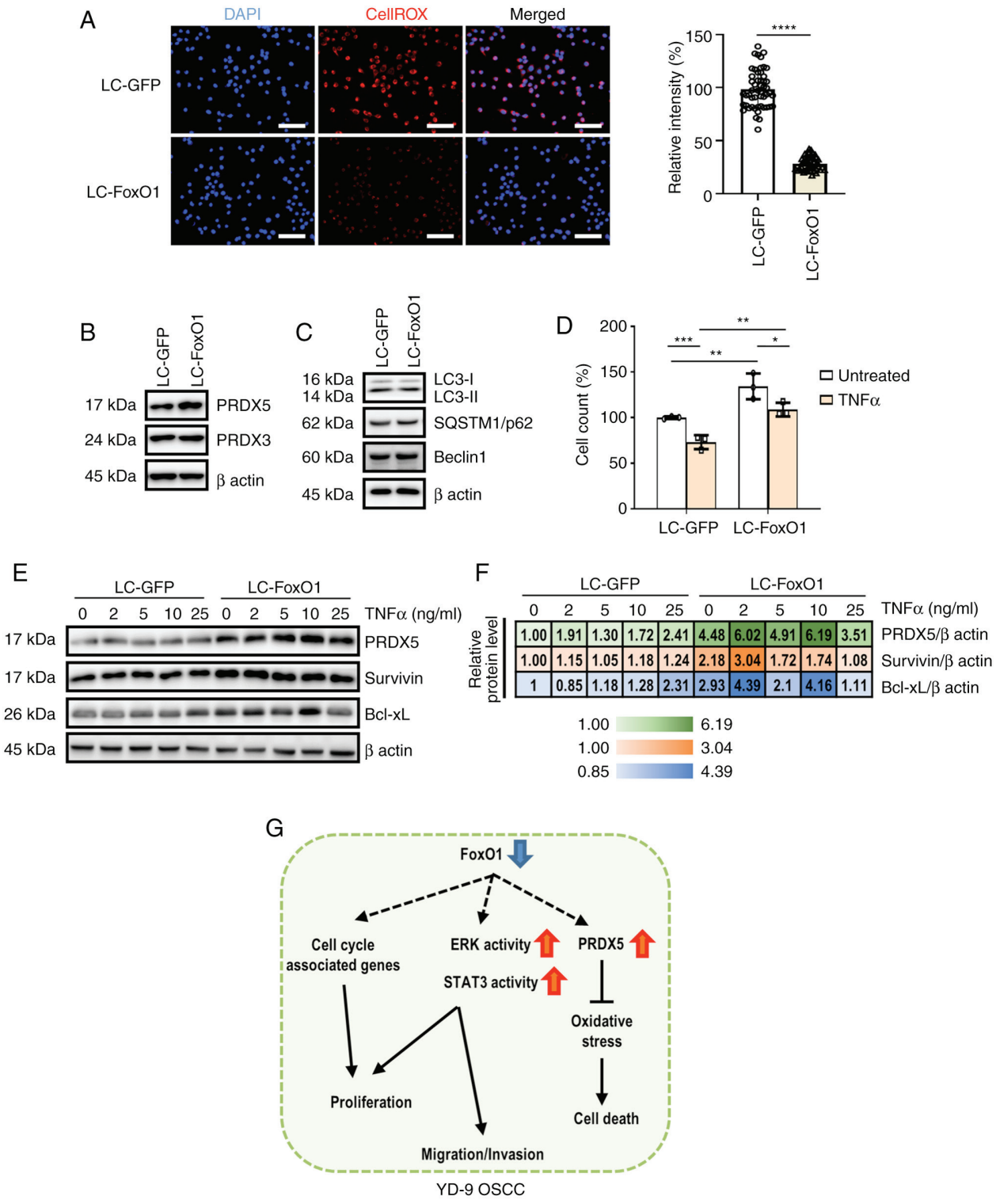

Figure 4. FoxO1 deficiency suppresses intracellular oxidative stress and death in YD-9 cells. (A) Control and FoxO1-deficient cells were subjected to CellROX staining. Nuclear DAPI signal is shown in blue. Scale bar, 100 μm. The relative CellROX signal intensities are shown. Immunoblot analysis of proteins involved in (B) reactive oxygen species scavenging and (C) autophagy response. (D) Relative cell numbers at 2 days after cell seeding in the presence or absence of 10 ng/ml TNFα treatment. (E) Immunoblot analysis of PRDX5, survivin, and Bcl-xL in control and FoxO1-deficient cells following treatment with TNFα for 2 days. β actin was used as a loading control. (F) Quantification of immunoblot analysis. (G) Proposed schematic of the anti-tumor properties of FoxO1 in YD-9 cells. FoxO1, forkhead transcriptional factor O1; PRDX5, peroxiredoxin 5; SQSTM1, sequestosome 1; OSCC, oral squamous cell carcinoma. *P<0.05, **P<0.01, ***P<0.001, ****P<0.0001.

has oncogenic properties: The cooperation of FoxO1 with β-catenin mediates hematopoiesis and induces malignant transformation of hematopoietic stem cells into leukemia cells (39). In ovarian cancer, cell viability and migration are disrupted by FoxO1 knockdown (40). Collectively, FoxO1 shows complicated molecular functions in cancer and thorough studies must be conducted into intra- and extracellular factors that affect these roles.

Given the importance of ERK and STAT3 signaling in tumor progression (28), the present study focused on their hyperactivation under FoxO1 silencing in this study. HIF1α protein levels were decreased in FoxO1-deficient YD-9 cells upon $CoCl_2$ treatment. Considering the tumor-promoting roles of HIF1α, decreased HIF1α in FoxO1-deficient cells with high proliferative and migratory capacity may appear contradictory. Although the present study did not assess HIF1α mRNA levels in the absence of FoxO1, FoxO1 may act as a transcription factor for Hif1α. Vasquez *et al* (41) demonstrated that HIF1α is a direct transcriptional target of FoxO1 and that HIF1α mRNA levels are decreased in human endometrial stromal cells when FoxO1 is silenced. In addition, intracellular redox status has a strong influence on HIF1α protein levels. Gao *et al* (42) demonstrated that N-Acetyl Cysteine significantly decreases HIF1α protein levels in human P493 B cells by lowering oxidative stress. Notably, the ROS scavenging protein PRDX5 has been shown to inhibit HIF1α stabilization and HIF activity (43). According to the present results, FoxO1 depletion led to the upregulation of PRDX5 protein levels and downregulation of oxidative stress, subsequently contributing to a decrease in HIF1α protein levels. Therefore, dysregulated ERK and STAT3 activation may override the effect of decreased HIF1α levels in FoxO1-deficient YD-9 cells.

Although the present study determined the molecular function of FoxO1 in YD-9 OSCC cells, the study has limitations. First, it did not determine why FoxO1 expression is elevated in a subset of oral cancer cell lines and patients with OSCC. Second, the roles of FoxO1 in other oral cancer cells infected with human papillomavirus or mutated p53 were not investigated. Given tumor heterogeneity, it is important to explore the molecular functions of FoxO1 in different types of tumor. Third, the detailed mechanism of FoxO1 knockdown-induced activation of ERK and STAT3 was not determined. Understanding the crosstalk between molecules and signaling pathways is key in tumor biology.

Based on the present results, further studies need to be performed. First, the molecular mechanisms of malignant transformation from OLP to OSCC need to be documented. OLP and OSCC share certain molecular features and cellular phenotypes. To explore the link between OLP and OSCC and to determine whether FoxO1 is implicated in disease progression is important for development of therapeutic strategies. In addition, it should be tested whether FoxO1 overexpression or activation suppresses or reverses the pathogenesis of OSCC. Several therapeutic options have been developed for the treatment of OSCC (44). Nonetheless, complete recovery from OSCC is not easy. Although further evaluations are required, the present results suggest FoxO1 activation as a potential therapeutic strategy against OSCC.

Acknowledgements

Not applicable.

Funding

The present study was supported by the National Research Foundation of Korea funded by the Korean government (grant nos. 2017R1A5A2015391, 2022R1C1C1006181 and 2020R1C1C1006757) and the Basic Science Research Program through the National Research Foundation of Korea funded by the Ministry of Education (grant no. 2019R1I1A2A01062430).

Availability of data and materials

The datasets and materials used in the current study are available from the corresponding author on reasonable request.

Authors' contributions

KHL, JSB and DYK conceived the study. YGK, CES, KAC, KHL, JSB and DYK wrote the manuscript. YGK, CES, KAC, SML, TJK, HJK and JHC performed the experiments. YGK, CES, KAC, SML, TJK, HJK, JHC, JCS, WJ, SJ, KHL, JSB and DYK designed the methodology. YGK, CES, KAC, KHL, JSB and DYK collected data. WJ, SJ, JCS and KHL provided resources. JSB and DYK obtained funding. YGK and DYK confirm the authenticity of all the raw data. All authors have read and approved the final manuscript.

Ethics approval and consent to participate

The present study was approved by the Institutional Review Board of Jeonbuk National University Hospital (approval no. CUH 2021-02-044-001), and written informed consent was obtained from all the participants.

Patient consent for publication

Not applicable.

Competing interests

The authors declare that they have no competing interests.

References

1. Rivera C: Essentials of oral cancer. Int J Clin Exp Pathol 8: 11884-11894, 2015.
2. Weckx A, Riekert M, Grandoch A, Schick V, Zöller JE and Kreppel M: Time to recurrence and patient survival in recurrent oral squamous cell carcinoma. Oral Oncol 94: 8-13, 2019.
3. Omar E: Current concepts and future of noninvasive procedures for diagnosing oral squamous cell carcinoma-a systematic review. Head Face Med 11: 6, 2015.
4. Safi AF, Kauke M, Grandoch A, Nickenig HJ, Zöller JE and Kreppel M: Analysis of clinicopathological risk factors for locoregional recurrence of oral squamous cell carcinoma-retrospective analysis of 517 patients. J Craniomaxillofac Surg 45: 1749-1753, 2017.
5. Collado M and Serrano M: Senescence in tumours: Evidence from mice and humans. Nat Rev Cancer 10: 51-57, 2010.
6. Hanahan D and Weinberg RA: Hallmarks of cancer: The next generation. Cell 144: 646-674, 2011.
7. Yadav RK, Chauhan AS, Zhuang L and Gan B: FoxO transcription factors in cancer metabolism. Semin Cancer Biol 50: 65-76, 2018.
8. Chae YC, Kim JY, Park JW, Kim KB, Oh H, Lee KH and Seo SB: FOXO1 degradation via G9a-mediated methylation promotes cell proliferation in colon cancer. Nucleic Acids Res 47: 1692-1705, 2019.
9. Dong T, Zhang Y, Chen Y, Liu P, An T, Zhang J, Yang H, Zhu W and Yang X: FOXO1 inhibits the invasion and metastasis of hepatocellular carcinoma by reversing ZEB2-induced epithelial-mesenchymal transition. Oncotarget 8: 1703-1713, 2017.

10. Furuyama T, Kitayama K, Shimoda Y, Ogawa M, Sone K, Yoshida-Araki K, Hisatsune H, Nishikawa S, Nakayama K, Nakayama K, *et al*: Abnormal angiogenesis in Foxo1 (Fkhr)-deficient mice. J Biol Chem 279: 34741-34749, 2004.
11. Cancer Genome Atlas Research Network: The molecular taxonomy of primary prostate cancer. Cell 163: 1011-1025, 2015.
12. Trinh DL, Scott DW, Morin RD, Mendez-Lago M, An J, Jones SJ, Mungall AJ, Zhao Y, Schein J, Steidl C, *et al*: Analysis of FOXO1 mutations in diffuse large B-cell lymphoma. Blood 121: 3666-3674, 2013.
13. Hornsveld M, Smits LMM, Meerlo M, van Amersfoort M, Groot Koerkamp MJA, van Leenen D, Kloet DEA, Holstege FCP, Derksen PWB, Burgering BMT and Dansen TB: FOXO transcription factors both suppress and support breast cancer progression. Cancer Res 78: 2356-2369, 2018.
14. Sanjana NE, Shalem O and Zhang F: Improved vectors and genome-wide libraries for CRISPR screening. Nat Methods 11: 783-784, 2014.
15. van der Meij EH and van der Waal I: Lack of clinicopathologic correlation in the diagnosis of oral lichen planus based on the presently available diagnostic criteria and suggestions for modifications. J Oral Pathol Med 32: 507-512, 2003.
16. Livak KJ and Schmittgen TD: Analysis of relative gene expression data using real-time quantitative PCR and the 2(-Delta Delta C(T)) method. Methods 25: 402-408, 2001.
17. Shi W, Yang J, Li S, Shan X, Liu X, Hua H, Zhao C, Feng Z, Cai Z, Zhang L and Zhou D: Potential involvement of miR-375 in the premalignant progression of oral squamous cell carcinoma mediated via transcription factor KLF5. Oncotarget 6: 40172-40185, 2015.
18. Cerami E, Gao J, Dogrusoz U, Gross BE, Sumer SO, Aksoy BA, Jacobsen A, Byrne CJ, Heuer ML, Larsson E, *et al*: The cBio cancer genomics portal: An open platform for exploring multidimensional cancer genomics data. Cancer Discov 2: 401-404, 2012.
19. Gao J, Aksoy BA, Dogrusoz U, Dresdner G, Gross B, Sumer SO, Sun Y, Jacobsen A, Sinha R, Larsson E, *et al*: Integrative analysis of complex cancer genomics and clinical profiles using the cBioPortal. Sci Signal 6: pl1, 2013.
20. Tang Z, Li C, Kang B, Gao G, Li C and Zhang Z: GEPIA: A web server for cancer and normal gene expression profiling and interactive analyses. Nucleic Acids Res 45 (W1): W98-W102, 2017.
21. Lee EJ, Kim J, Lee SA, Kim EJ, Chun YC, Ryu MH and Yook JI: Characterization of newly established oral cancer cell lines derived from six squamous cell carcinoma and two mucoepidermoid carcinoma cells. Exp Mol Med 37: 379-390, 2005.
22. Ashburner M, Ball CA, Blake JA, Botstein D, Butler H, Cherry JM, Davis AP, Dolinski K, Dwight SS, Eppig JT, *et al*: Gene ontology: Tool for the unification of biology. The gene ontology consortium. Nat Genet 25: 25-29, 2000.
23. Gene Ontology Consortium: The gene ontology resource: Enriching a GOld mine. Nucleic Acids Res 49 (D1): D325-D334, 2021.
24. Mi H, Muruganujan A, Ebert D, Huang X and Thomas PD: PANTHER version 14: More genomes, a new PANTHER GO-slim and improvements in enrichment analysis tools. Nucleic Acids Res 47 (D1): D419-D426, 2019.
25. Birkenkamp-Demtröder K, Hahn SA, Mansilla F, Thorsen K, Maghnouj A, Christensen R, Øster B and Ørntoft TF: Keratin23 (KRT23) knockdown decreases proliferation and affects the DNA damage response of colon cancer cells. PLoS One 8: e73593, 2013.
26. Sequeira I and Watt FM: The role of keratins in modulating carcinogenesis via communication with cells of the immune system. Cell Stress 3: 136-138, 2019.
27. Wu H, Wang K, Liu W and Hao Q: PTEN overexpression improves cisplatin-resistance of human ovarian cancer cells through upregulating KRT10 expression. Biochem Biophys Res Commun 444: 141-146, 2014.
28. Gkouveris I, Nikitakis N, Karanikou M, Rassidakis G and Sklavounou A: Erk1/2 activation and modulation of STAT3 signaling in oral cancer. Oncol Rep 32: 2175-2182, 2014.
29. Saxena NK, Sharma D, Ding X, Lin S, Marra F, Merlin D and Anania FA: Concomitant activation of the JAK/STAT, PI3K/AKT, and ERK signaling is involved in leptin-mediated promotion of invasion and migration of hepatocellular carcinoma cells. Cancer Res 67: 2497-2507, 2007.
30. Ponugoti B, Xu F, Zhang C, Tian C, Pacios S and Graves DT: FOXO1 promotes wound healing through the up-regulation of TGF-β1 and prevention of oxidative stress. J Cell Biol 203: 327-343, 2013.
31. Kesarwala AH, Krishna MC and Mitchell JB: Oxidative stress in oral diseases. Oral Dis 22: 9-18, 2016.
32. Olmos Y, Sánchez-Gómez FJ, Wild B, García-Quintans N, Cabezudo S, Lamas S and Monsalve M: SirT1 regulation of antioxidant genes is dependent on the formation of a FoxO3a/PGC-1α complex. Antioxid Redox Signal 19: 1507-1521, 2013.
33. Wang Q, Sztukowska M, Ojo A, Scott DA, Wang H and Lamont RJ: FOXO responses to Porphyromonas gingivalis in epithelial cells. Cell Microbiol 17: 1605-1617, 2015.
34. Filomeni G, De Zio D and Cecconi F: Oxidative stress and autophagy: The clash between damage and metabolic needs. Cell Death Differ 22: 377-388, 2015.
35. Zhao H, Wu L, Yan G, Chen Y, Zhou M, Wu Y and Li Y: Inflammation and tumor progression: Signaling pathways and targeted intervention. Signal Transduct Target Ther 6: 263, 2021.
36. Xie L, Ushmorov A, Leithäuser F, Guan H, Steidl C, Färbinger J, Pelzer C, Vogel MJ, Maier HJ, Gascoyne RD, *et al*: FOXO1 is a tumor suppressor in classical Hodgkin lymphoma. Blood 119: 3503-3511, 2012.
37. Duan X, Kong Z, Liu Y, Zeng Z, Li S, Wu W, Ji W, Yang B, Zhao Z and Zeng G: β-Arrestin2 contributes to cell viability and proliferation via the down-regulation of FOXO1 in castration-resistant prostate cancer. J Cell Physiol 230: 2371-2381, 2015.
38. Lin A, Yao J, Zhuang L, Wang D, Han J, Lam EW and Gan B: The FoxO-BNIP3 axis exerts a unique regulation of mTORC1 and cell survival under energy stress. Oncogene 33: 3183-3194, 2014.
39. Kode A, Mosialou I, Manavalan SJ, Rathinam CV, Friedman RA, Teruya-Feldstein J, Bhagat G, Berman E and Kousteni S: FoxO1-dependent induction of acute myeloid leukemia by osteoblasts in mice. Leukemia 30: 1-13, 2016.
40. Han GH, Chay DB, Nam S, Cho H, Chung JY and Kim JH: Prognostic implications of forkhead box protein O1 (FOXO1) and paired box 3 (PAX3) in epithelial ovarian cancer. BMC Cancer 19: 1202, 2019.
41. Vasquez YM, Mazur EC, Li X, Kommagani R, Jiang L, Chen R, Lanz RB, Kovanci E, Gibbons WE and DeMayo FJ: FOXO1 is required for binding of PR on IRF4, novel transcriptional regulator of endometrial stromal decidualization. Mol Endocrinol 29: 421-433, 2015.
42. Gao P, Zhang H, Dinavahi R, Li F, Xiang Y, Raman V, Bhujwalla ZM, Felsher DW, Cheng L, Pevsner J, *et al*: HIF-dependent antitumorigenic effect of antioxidants in vivo. Cancer Cell 12: 230-238, 2007.
43. Sabharwal SS, Waypa GB, Marks JD and Schumacker PT: Peroxiredoxin-5 targeted to the mitochondrial intermembrane space attenuates hypoxia-induced reactive oxygen species signalling. Biochem J 456: 337-346, 2013.
44. Dwivedi R, Pandey R, Chandra S and Mehrotra D: Dendritic cell-based immunotherapy: A potential player in oral cancer therapeutics. Immunotherapy 15: 457-469, 2023.